ELSEVIER

Chemical Engineering Journal 132 (2007) 267–278

Chemical Engineering Journal

www.elsevier.com/locate/cej

Adsorption thermodynamics and isosteric heat of adsorption of toxic metal ions onto bagasse fly ash (BFA) and rice husk ash (RHA)

Vimal Chandra Srivastava [a,*], Indra Deo Mall [b,*], Indra Mani Mishra [b]

[a] *Department of Chemical Engineering and Technology, Institute of Technology, Banaras Hindu University, Varanasi 221005, Uttar Pradesh, India*
[b] *Department of Chemical Engineering, Indian Institute of Technology Roorkee, Roorkee 247667, Uttaranchal, India*

Received 8 April 2006; received in revised form 2 January 2007; accepted 5 January 2007

Abstract

The equilibrium sorption characteristics of cadmium (Cd(II)), nickel (Ni(II)) and zinc (Zn(II)) metal ions from aqueous solutions having respective metal ion concentrations in the range of 50–500 mmol/dm^3 for two low-cost adsorbents, viz. bagasse fly ash (BFA) and rice husk ash (RHA), were studied at different temperatures in the range of 293–323 K. An increase in temperature is found to induce a positive effect on the sorption process. Toth isotherm best represents the equilibrium adsorption onto BFA and RHA. The heat of adsorption (ΔH_0) and change in entropy (ΔS_0) for metal adsorption on BFA and RHA are found in the range of 26–44 kJ/mol and 127–194 kJ/mol K, respectively. The isosteric heat of adsorption was quantitatively correlated with the fractional loading of metal ions onto adsorbents. The results showed that the BFA and RHA possessed heterogeneous surface with sorption sites having different activities.

Keywords: Adsorption; Toxic metal removal; Thermodynamics; Temperature; Isotherms; Isosteric heat of adsorption

1. Introduction

Adsorption has attracted considerable interest in recent years as a wastewater treatment process. Equilibrium adsorption isotherms and isosteric enthalpy are the basic requirements for the characterization and development of adsorbents and the optimization of the sorption process. The isosteric heat of adsorption is a critical design variable in estimating the performance of an adsorptive separation process. The heat of adsorption can be a strong and a complex function of the adsorbate loading when the adsorbent is energetically heterogeneous. Generally, sorption isosteric enthalpy varies with the change in adsorption loading when organic compounds are adsorbed onto adsorbents [1,2]. It also gives some indication about the surface energetic heterogeneity [3]. The complexity of the adsorption phenomena occurring at the liquid/solid interfaces have led to a few investigations on the subject matter [4,5].

The release of the industrial effluents containing toxic metals into the receiving water bodies is a matter of profound environmental concern. The removal of toxic metals from industrial effluents so that their residual concentrations conform to the effluent standards, is statutorily mandatory [6]. Metal ions like cadmium (Cd(II)), nickel (Ni(II)) and zinc (Zn(II)) are toxic, and are frequently encountered together in waste waters (from mine drainage, metal plating plants, paint and ink formulation units, porcelain enamelling, etc.).

The toxic effects of heavy metals have been described in several books and research papers [6–8]. Although, Zn(II) is not especially hazardous, but its association with toxic Cd(II) as an impurity makes it a critical metal ion for its removal [8]. The Ministry of Environment and Forests, Government of India has prescribed Minimal National Standards, MINAS, of 0.2, 2.0 and 5.0 mg/dm^3, respectively, for the discharge of Cd(II), Ni(II) and Zn(II) containing effluents into surface waters [9]. The permissible Cd(II), Ni(II) and Zn(II) concentrations in potable waters have been set as 0.003, 0.02 and 3 mg/dm^3 [10].

Adsorption using activated carbon has been found to be an attractive process for the removal of heavy metals from industrial effluents. However, the cost of activated carbon and the loss of adsorption efficiency after regeneration of the exhausted activated carbon have limited its use in effluent wastewater treatment. Therefore, alternative low-cost, non-conventional adsorbents such as bagasse fly ash (BFA), rice husk ash (RHA),

* Corresponding authors. Tel.: +91 542 2307045; fax: +91 542 2368092/428.
E-mail addresses: vimalcsr@yahoo.co.in (V.C. Srivastava), id_mall2000@yahoo.co.in (I.D. Mall), imishfch@iitr.ac.in (I.M. Mishra).

1385-8947/$ – see front matter © 2007 Elsevier B.V. All rights reserved.
doi:10.1016/j.cej.2007.01.007

peat, lignite, bagasse pith, wood, saw dust, etc. have been investigated for the treatment of effluents. Rice husk is an agricultural waste used as a fuel in the steam boilers. Bagasse is available in plenty from the cane sugar mills and is used as a fuel in the boilers. RHA and BFA are collected from the particulate collection devices attached downstream to the boiler furnaces and upstream to the flue gas stacks of the rice husk/bagasse fired boilers. BFA and RHA have been shown to be very effective adsorbents in the removal of COD and colour from paper mill effluents [11], and the removal of dyes [12,13], pyridine [14], phenol [15] and metal ions from aqueous solutions [16].

The present investigation deals with the adsorption thermodynamics and isosteric heat of adsorption of three heavy metal ions, namely, Cd(II), Ni(II) and Zn(II) from aqueous solutions using bagasse fly ash (BFA) and rice husk ash (RHA). The equilibrium sorption behaviour of the adsorbents has been studied using the adsorption isotherm technique. Experimental data were fitted to various isotherm equations to determine the best isotherm to correlate the experimental data. The effect of temperature on metal ions adsorption onto these adsorbents has also been investigated. Thermodynamics of adsorption process has been studied and the change in Gibbs free energy and the enthalpy have been determined.

2. Experimental

2.1. Adsorbents and their characterization

BFA and RHA were used as obtained without any pretreatment, except sieving, to remove very fine particles. BFA was obtained from Deoband Sugar Mill, Deoband, U.P., India. RHA was procured from Barnala Paper Mill, Punjab, India.

Proximate analysis and chemical analysis of the adsorbents were carried out as per IS 1350: 1984 and IS 355-1974, respectively [17,18]. Bulk density was determined by using MAC bulk density meter, whereas particle size analysis was carried out using standard sieves. X-ray diffraction analysis of BFA was carried out using Phillips (Holland) diffraction unit (Model PW 1140/90), using copper target with nickel as filter media, and K radiation maintained at 1.542 Å. Goniometer speed was maintained at 1°/min. The specific surface area was measured by N_2 adsorption isotherm using an ASAP 2010 Micromeritics instrument and by Brunauer–Emmett–Teller (BET) method, using the software of Micromeritics. Nitrogen was used as cold bath (77.15 K). The Barrett–Joyner–Halenda (BJH) method [19] was used to calculate the mesopore distribution for the BFA. FTIR spectrometer (Thermo nicolet, Model Magna 760) was employed to determine the presence of functional groups in BFA at room temperature. Pellet (pressed-disk) technique was used for this purpose. The pellets were prepared by using the same ratio of each adsorbent in KBr. The spectral range was from 4000 to 400 cm^{-1}.

2.2. Adsorbates

All the chemicals used in the study were of analytical reagent grade. Nickel chloride hexahydrate ($NiCl_2{\cdot}6H_2O$) was procured from Qualigens Fine Chemicals, Mumbai, India. Cadmium sulphate octahydrate ($3CdSO_4{\cdot}8H_2O$), zinc sulphate heptahydrate ($ZnSO_4{\cdot}7H_2O$), NaOH, HCl, HNO_3, H_2SO_4 and CH_3COOH were obtained from S.D. Fine Chemicals, Mumbai. Stock solutions of 1 g/dm^3 strength of Cd(II), Ni(II) and Zn(II) metal ions were prepared by dissolving exact amount of $3CdSO_4{\cdot}8H_2O$, $NiCl_2{\cdot}6H_2O$ and $ZnSO_4{\cdot}7H_2O$ separately in double-distilled water. The stock solution for each metal salt was diluted to give metal ion concentration in the range of 50–500 mg/dm^3 for use in the experiments.

2.3. Batch adsorption studies

For each experimental run, 100 ml aqueous solution of a known concentration of one of the metal ions was taken in a 250 ml conical flask containing 1 g of adsorbent. These flasks were agitated at a constant shaking rate of 150 rpm in a temperature controlled orbital shaker (Remi Instruments, Mumbai) maintained at 293, 303, 313 or 323 K. The initial pH (pH_0) of the adsorbate solution was adjusted to 6.0 using 1N HCl or 1N NaOH aqueous solution without any further adjustment during the sorption process. The pH of the solution was monitored during the course of the sorption process using a pH meter. The equilibrium was found to have been attained in 5 h contact time. The samples withdrawn after 5 h were centrifuged using Research Centrifuge (Remi Instruments, Mumbai) at 5000 rpm for 5 min and then the supernatant liquid was analyzed for the residual concentration of metal ions.

The removal of metal ions from the solution and the equilibrium adsorption uptake in the solid phase, q_e (mmol/g), were calculated using the following relationships:

$$\%\ \text{adsorbate removal} = \frac{C_0 - C_e}{C_0} \times 100 \quad (1)$$

$$q_e = \frac{(C_0 - C_e)V}{w} \quad (2)$$

where C_0 is the initial metal ion concentration (mmol/dm^3), C_e the equilibrium metal ion concentration (mmol/dm^3), V the volume of the solution (dm^3) and w is the mass of the adsorbent (g).

2.4. Analysis of metal ions

The concentration of Cd(II), Ni(II) and Zn(II) ions in the aqueous samples was determined using a flame atomic absorption spectrophotometer (GBC Avanta, Australia) with the detection limit of 0.009, 0.040 and 0.008 mg/dm^3 at the wavelength of 228.8 nm, 232 nm and 213.9 nm, for Cd(II), Ni(II) and Zn(II), respectively, by using air–acetylene flame. Before the analysis, the sample was diluted, if necessary, with distilled water to a concentration in the range of 0.2–1.8 mg/dm^3 for Cd(II), 1.8–8 mg/dm^3 for Ni(II) and 0.4–1.5 mg/dm^3 for Zn(II). Metal ion concentrations were determined with reference to the appropriate standard metal ion solutions. The mass concentrations were converted into molar concentrations.

2.5. Effect of temperature and estimation of thermodynamic parameters

The effect of temperature on the sorption characteristics was investigated by determining the adsorption isotherms at 293, 303, 313 or 323 K. Apparent and net isosteric heats of adsorption at various surface coverages have been determined using the classical thermodynamic equations. C_0 was varied in the range of 50–500 mg/dm^3, thus giving different molar concentrations for each metal.

2.6. Batch adsorption isotherm study and error analysis

Batch experiments were carried out by contacting a fixed amount of adsorbent with 100 ml of the respective metal solution. After 5 h contact time, samples were withdrawn and centrifuged and the residual metal concentration in the supernatant was determined. The equilibrium sorption data were fitted to the Langmuir, Freundlich, Temkin, Redlich–Peterson and Toth isotherm equations to test the applicability and adequacy of these equations for metal ions adsorption onto BFA and RHA.

The Marquardt's percent standard deviation (MPSD) error function [20], was used to test the adequacy of the isotherm equations to represent the experimental data. This error function is given as:

$$\mathrm{MPSD} = 100\sqrt{\frac{1}{n-p}\sum_{i=1}^{n}\left(\frac{(q_{e,meas}-q_{e,calc})}{q_{e,meas}}\right)_i^2} \quad (3)$$

The MPSD accounts for the number of degrees of freedom of the system, and is similar in some respects to a geometric mean error distribution.

3. Results and discussion

3.1. Characterization of adsorbents

Detailed physico-chemical characteristics of BFA have been presented by the authors recently [12,15]. Srivastava et al. [21] have presented detailed physico-chemical properties of RHA. Table 1 shows the properties of BFA and RHA. The bulk density of RHA is found to be lower than that of BFA. Proximate analysis showed presence of 19.20% and 5.90% fixed carbon in BFA and RHA, respectively. Thus, BFA shows higher percentage of carbon. This was confirmed by the CHN analysis of adsorbents that showed 16.36% and 7.42% carbon in BFA and RHA, respectively. Due to presence of high carbon content, BFA can be treated as more organic in nature. Because of this, BFA will have much higher porosity and surface area.

The shape of adsorption isotherms can provide qualitative information on the adsorption process and the extent of the surface area available to the adsorbate. Based on an extensive literature survey, Brunauer et al. [22] found that all the adsorption isotherms would fit into one of five basic types (Types I–V). For a specific type of adsorption isotherm, the adsorbent is supposed to have certain porosity. The isotherm of nitrogen adsorption/desorption at 77.15 K for BFA and RHA are of Type IV, indicating mesoporous structure of BFA and RHA [23].

Table 1
Characteristics of BFA and RHA

Characteristics	BFA	RHA
Proximate analysis		
Moisture (%)	3.39	0.73
Ash (%)	72.60	88.0
Volatile matter (%)	4.81	5.37
Fixed carbon (%)	19.20	5.90
Chemical analysis of ash		
Insoluble	78.35	75.17
SiO_2 (%)	2.46	2.60
Fe_2O_3 & Al_2O_3 (%)	2.92	3.38
CaO (%)	14.00	17.40
MgO (%)	1.09	0.96
Rest others	1.18	0.49
Bulk density (kg/m^3)	185.51	104.9
Heating value (kJ/kg)	4.63	9.68
Average particle size (μm)	167.35	150.47
CHN analysis		
C (%)	16.36	7.42
H (%)	9.77	0.06
N (%)	2.55	0.85
Surface area of pores (m^2/g)		
(i) BET	168.39	36.44
(ii) BJH		
(a) Adsorption cumulative	70.90	27.45
(b) Desorption cumulative	45.30	22.18
BJH cumulative pore volume (cm^3/g)		
(i) Single point total	0.1067	0.0388
(ii) BJH adsorption	0.0844	0.0386
(iii) BJH desorption	0.0622	0.0352
Average pore diameter (Å)		
(i) BET	25.54	42.60
(ii) BJH adsorption	49.85	56.22
(iii) BJH desorption	58.44	63.35
XRD	Alumina (Al_2O_3); $CaSiO_3$; $Ca_8Si_5O_{18}$; amorphous silica	Cristobalite (SiO_2); margaritasite ($(Cs,K,H_3O)_2(UO_2)2V_2O_8\cdot(H_2O)$); macedonite ($PbTiO_3$)

BFA and RHA have a wide pore size distribution (Fig. 1) giving a wide distribution of surface area. The BET surface area of BFA and RHA are found to be 168.39 and 36.44 m^2/g, respectively. RHA has larger pore sizes than BFA and the BET average pore diameters are 25.54 and 42.60 Å, respectively. Thus, the BFA has shows higher surface area and pore volume than RHA. The analysis of the BJH adsorption pore distribution of RHA shows that the micropores ($d < 20$ Å) have a total pore area of about 20%, mesopores (20 Å $< d <$ 500 Å) account for about 78% and that the macropores ($d > 500$ Å) about 2% [24]. Mesopores account for more than 99% of the total pore area in the BFA. Thus, it can be concluded that the BFA and RHA are predominantly mesoporous. This is what is desirable for the liquid phase adsorption of metal ions.

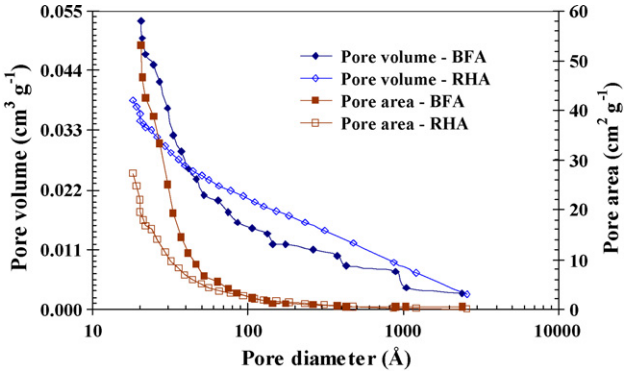

Fig. 1. Pore size distribution of BFA and RHA.

The *d*-spacing values as obtained from the X-ray spectra of BFA and RHA reflect the presence of different major components in the adsorbents (Table 1). Diffraction peaks corresponding to crystalline carbon are not found in both the adsorbents, whereas, amorphous form of silica is identified in both the adsorbents.

FTIR spectra for both the adsorbents show a broad band between 3100 and 3700 cm^{-1} for both the adsorbents (Fig. 2). This indicates the presence of both free and hydrogen bonded OH groups on the adsorbent surface [25]. This stretching is due to both the silanol groups (Si–OH) and adsorbed water (peak at 3400 cm^{-1}) on the surface [26]. The stretching of the OH groups bound to methyl radicals presented a very light signal ~2920 cm^{-1} for BFA. The IR spectra of both the adsorbents indicated weak and broad peaks in the region of 1600–1800 cm^{-1} corresponding to CO group stretching from aldehydes and ketones. The band at 1600 cm^{-1} may be due to conjugated hydrocarbon bonded carbonyl groups. The FTIR spectra showed transmittance at 1100 cm^{-1} due to the vibration of the CO group in lactones [27]. The 1360–1420 cm^{-1} band in BFA and RHA may be attributed to the aromatic CH and carboxyl-carbonate structures [28]. Although some inference can be drawn about the surface functional groups from IR spectra, the weak and broad bands do not provide any authentic information about the nature of the surface oxides. The presence of polar groups on the surface is likely to give considerable cation exchange capacity to the adsorbents. The surface structures of carbon–oxygen (functional groups) are by far the most important structures in influencing the surface characteristics and surface behaviour of carbon.

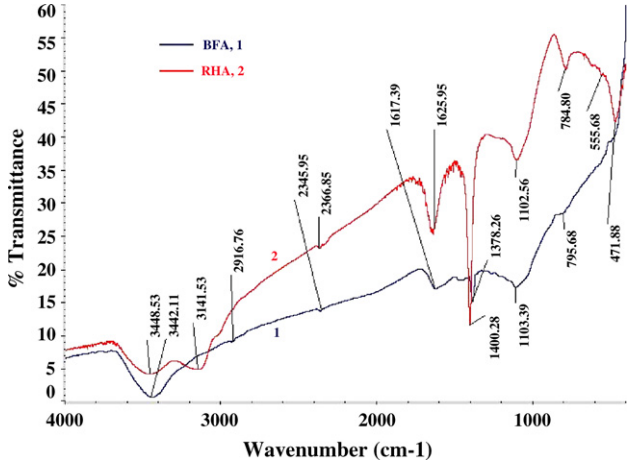

Fig. 2. FTIR spectroscopy of BFA and RHA.

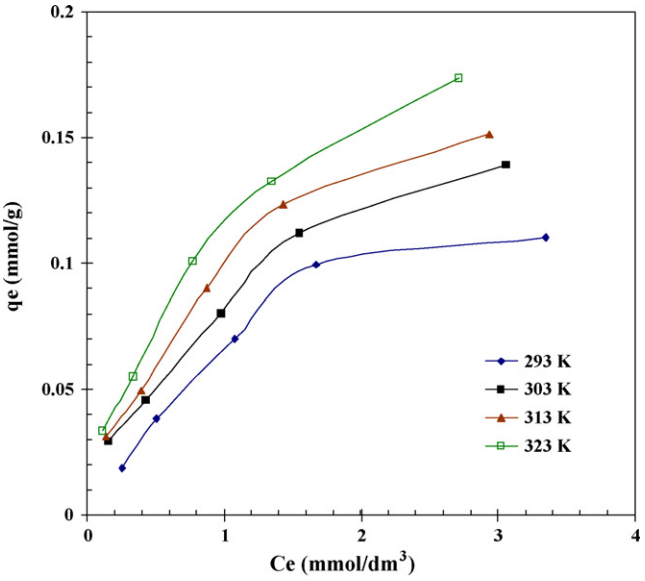

Fig. 3. Equilibrium adsorption isotherms at different temperature for Cd(II)–BFA system (pH$_0$: 6.0; *m*: 10 g/dm^3).

3.2. *Effect of temperature and initial metal ion concentration*

Temperature has a pronounced effect on the adsorption capacity of the adsorbents. Figs. 3 and 4 show the representative plots of adsorption isotherms, q_e versus C_e for Cd(II)–BFA and Cd(II)–RHA systems at different temperatures ranging from 293 to 323 K. It is found that the sorption of Cd(II) increases

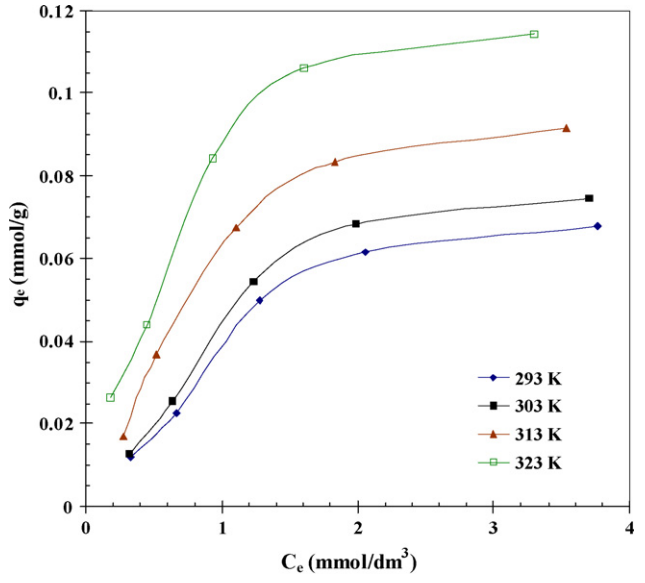

Fig. 4. Equilibrium adsorption isotherms at different temperature for Cd(II)–RHA system (pH$_0$: 6.0; *m*: 10 g/dm^3).

with an increase in temperature. At low adsorbate concentrations, q_e rises sharply. At higher values of C_e, the increase in q_e is gradual. Similar trends were observed for the sorption of Ni(II) and Zn(II) also. Since sorption is an exothermic process, it would be expected that an increase in temperature would result in a decrease in the sorption capacity of the adsorbent. However, if the adsorption process is controlled by the diffusion process (intraparticle transport-pore diffusion), the sorption capacity will increase with an increase in temperature due to endothermicity of the diffusion process. An increase in temperature results in an increased mobility of the metal ions and a decrease in the retarding forces acting on the diffusing ions. These result in the enhancement in the sorptive capacity of the adsorbents. However, the diffusion of the metal ions into the pores of the adsorbent is not the only rate-controlling step [15], and the diffusion resistance can be ignored with adequate contact time. Therefore, the increase in sorptive uptake of the metal ions with an increase in temperature may be attributed to chemisorption. In our earlier studies, it has been shown that the desorption of metal ions from the spent (loaded) BFA and RHA using various solvents (acids, bases and water) is not significant [16,21]. This confirms chemisorptive nature of adsorption.

There are various possible interaction effects between different species in solution and, in particular, potential interactions on the surface depending on the adsorption mechanism. Factors that affect the preference for an adsorbate may be related to the characteristics of the binding sites (e.g. functional groups, structure, surface properties, etc.), the properties of the adsorbates (e.g. concentration, ionic size, ionic weight, ionic charge, molecular structure, ionic nature or standard redox potential, etc.) and the solution chemistry (e.g. pH, ionic strength, etc.). In the context of adsorption, a number of properties have been suggested for use in the ordering of affinity rank, including ionic radius and solubility product constant as hydroxides [29]; Pauling electronegativity and standard reduction potential [30]; first hydrolysis constant [31]. These properties may play an important role in metal ion-adsorbent interaction, but can only partly explain high- or low-adsorption capacities.

It is clear that each of the three metal ions is very easily adsorbed onto BFA and RHA. However, the affinity and adsorption capacity of each metal ion are different. The maximum adsorption capacity as calculated from the experimental data by fitting Toth isotherm Eq. (9) (given later) are shown in Tables 2 and 3. The atomic weight of Cd is highest as compared to Ni and Zn and the ionic radius of Cd(II) is highest (0.83 Å) as compared to Zn(II) (0.74 Å) and Ni(II) (0.73 Å). Both the tested adsorbents showed higher adsorption capacity for Ni(II) and Zn(II) ions as compared to Cd(II). Identification of a common denominator from the physical and chemical properties of Cd(II), Ni(II) and Zn(II) to check their interactive effects on the selective sorption of an adsorbate onto an adsorbent seems to be difficult at the moment. However, the adsorption order is found to be in the order of increasing molecular weight and ionic radius, i.e. Ni(II) > Zn(II) > Cd(II). The micro- and meso-pore size distribution of an adsorbent and the shape of the pores coupled with ionic size of the adsorbate play important roles in the adsorption uptake of the adsorbate. While considering adsorption characteristics, the minimum ionic size of the metal ion in one-dimension is critical for an adsorbent with slit shaped pores. In the case of an adsorbent having cylindrical pores with circular cross-section, the minimum ionic sizes in two-dimensions need to be considered.

An increase in C_0 increases the equilibrium uptake of the adsorbate by the adsorbent and decreases the percent removal of the adsorbate. The initial concentration provides the necessary driving force to overcome the resistances to the mass transfer of metal ions between the aqueous solution and the solid phase. The increase in C_0 also enhances the interaction between the metal ions in the aqueous phase and the adsorbents. Therefore, an increase in the C_0 of the metal ions enhances the adsorption uptake of Cd(II), Ni(II) and Zn(II) ions onto BFA and RHA.

3.3. Adsorption equilibrium study

The experimental equilibrium adsorption data have been tested by using the two-parameter models of Freundlich, Langmuir, and Temkin; and the three-parameter Redlich–Peterson (R–P) and Toth equations.

The Freundlich isotherm [32] is valid for a heterogeneous adsorbent surface with a non-uniform distribution of heat of adsorption over the surface. The Langmuir isotherm [33], however, assumes that the sorption takes place at specific homogeneous sites within the adsorbent. The R–P isotherm can, however, be applied in homogenous as well as heterogeneous systems.

The R–P isotherm can be described as follows [34]:

$$q_e = \frac{K_R C_e}{1 + a_R C_e^{\beta}} \tag{4}$$

where K_R is the R–P isotherm constant (dm^3/g), a_R the R–P isotherm constant (dm^3/mmol), β the exponent having values between 0 and 1, C_e the equilibrium liquid phase concentration of the adsorbate (mmol/dm^3) and q_e is the equilibrium uptake of the adsorbate by the adsorbent (mmol/g).

For high adsorbate concentrations, Eq. (4) reduces to the Freundlich isotherm equation:

$$q_e = K_F C_e^{1/n} \tag{5}$$

where $K_F = K_R/a_R$ is the Freundlich constant (dm^3/mmol), and $1/\eta = 1 - \beta$ is the heterogeneity factor.

For $\beta = 1$, Eq. (4) reduces to the Langmuir isotherm equation:

$$q_e = \frac{q_m K_L C_e}{1 + K_L C_e} \tag{6}$$

where K_L ($=a_R$) is the Langmuir adsorption constant (dm^3/mmol) related to the energy of adsorption, and q_m ($=K_R/a_R$) signifies adsorption capacity of the adsorbent (mmol/g).

For $\beta = 0$, Eq. (4) reduces to the Henry's equation, i.e.,

$$q_e = K_H C_e \tag{7}$$

where K_L ($=K_R$) is the Henry's constant (dm^3/g).

Table 2
Isotherm parameters for metal ions adsorption onto BFA at different temperatures

Temperature (K)	Cd(II)–BFA				Ni(II)–BFA				Zn(II)–BFA			
	K_F [(mmol/g)/(mmol/dm^3)$^{1/n}$]	$1/n$	R^2	MPSD	K_F [(mmol/g)/(mmol/dm^3)$^{1/n}$]	$1/n$	R^2	MPSD	K_F [(mmol/g)/(mmol/dm^3)$^{1/n}$]	$1/n$	R^2	MPSD
Freundlich												
293	0.0580	0.7119	0.9362	25.7104	0.0906	0.6639	0.9611	19.7996	0.1044	0.6543	0.9631	19.1101
303	0.0800	0.5494	0.9879	10.6273	0.1295	0.5241	0.9975	8.7632	0.1406	0.5053	0.9975	8.8199
313	0.0913	0.5445	0.9821	13.1129	0.1465	0.5402	0.9858	12.0850	0.1727	0.4342	0.9898	18.5808
323	0.1077	0.5322	0.9924	8.0844	0.1756	0.4751	0.9886	12.5516	0.2098	0.3786	0.9912	14.2360

Temperature (K)	Cd(II)–BFA				Ni(II)–BFA				Zn(II)–BFA			
	q_m (mmol/g)	K_L (dm^3/mmol)	R^2	MPSD	q_m (mmol/g)	K_L (dm^3/mmol)	R^2	MPSD	q_m (mmol/g)	K_L (dm^3/mmol)	R^2	MPSD
Langmuir												
293	0.1793	0.5449	0.9806	16.1651	0.3816	0.3495	0.9920	9.0710	0.3796	0.4379	0.9949	8.6514
303	0.1885	0.8936	0.9913	19.9489	0.4074	0.5222	0.9881	24.7687	0.3865	0.6760	0.9840	26.9892
313	0.2006	1.0302	0.9921	20.3378	0.4262	0.6247	0.9952	18.3622	0.3925	0.9965	0.9779	40.5365
323	0.2248	1.1554	0.9933	17.1771	0.4316	0.8623	0.9886	28.4313	0.3992	1.5972	0.9750	45.3960

Temperature (K)	Cd(II)–BFA				Ni(II)–BFA				Zn(II)–BFA			
	K_T (dm^3/mmol)	B_1	R^2	MPSD	K_T (dm^3/mmol)	B_1	R^2	MPSD	K_T (dm^3/mmol)	B_1	R^2	MPSD
Temkin												
293	6.1045	0.0383	0.9856	14.1782	3.8684	0.0811	0.9902	15.6776	4.8733	0.0805	0.9918	21.4645
303	10.7504	0.0382	0.9751	32.9202	6.9893	0.0787	0.9682	37.1376	9.4833	0.0734	0.9654	37.7528
313	12.2630	0.0409	0.9770	33.6649	12.1265	0.0824	0.9825	47.8226	18.0339	0.0688	0.9525	47.1190
323	14.6606	0.0445	0.9779	28.2095	14.6606	0.0445	0.9732	67.3718	37.8261	0.0649	0.9566	42.9095

Temperature (K)	Cd(II)–BFA					Ni(II)–BFA					Zn(II)–BFA				
	K_R (dm^3/g)	a_R (dm^3/mmol)	β	R^2	MPSD	K_R (dm^3/g)	a_R (dm^3/mmol)	β	R^2	MPSD	K_R (dm^3/g)	a_R (dm^3/mmol)	β	R^2	MPSD
R–P															
293	0.0894	0.4402	0.9990	0.9750	14.3582	0.1271	0.3133	0.9990	0.9905	8.2431	0.1586	0.3943	0.9990	0.9935	7.8242
303	0.1600	0.8435	0.9990	0.9923	20.5146	0.2150	0.5692	0.9490	0.9911	24.1481	0.2963	0.9411	0.8903	0.9881	23.7725
313	0.2000	1.0217	0.9608	0.9932	20.3559	0.2461	0.5347	0.9990	0.9969	19.9613	0.5028	1.7544	0.8009	0.9870	34.8713
323	0.2552	1.1330	0.9786	0.9948	21.1742	0.3596	0.8871	0.9654	0.9913	28.3356	0.8379	2.6536	0.8405	0.9855	39.1921

Temperature (K)	Cd(II)–BFA					Ni(II)–BFA					Zn(II)–BFA				
	q_e^∞ (mmol/g)	K_{Th} [(mmol/dm^3)Th]	Th	R^2	MPSD	q_e^∞ (mmol/g)	K_{Th} [(mmol/dm^3)Th]	Th	R^2	MPSD	q_e^∞ (mmol/g)	K_{Th} [(mmol/dm^3)Th]	Th	R^2	MPSD
Toth															
293	0.2060	2.2723	0.9872	0.9747	14.4616	0.3101	4.6001	1.5458	0.9955	7.7745	0.3091	3.2259	1.4836	0.9983	6.3007
303	0.3332	1.1020	0.5406	0.9933	9.3382	0.4430	1.1105	0.6454	0.9858	8.5833	0.4267	0.8773	0.6059	0.9822	8.9876
313	0.3539	1.1320	0.5850	0.9923	12.7674	0.4908	1.2132	0.7080	0.9951	12.8335	0.4462	0.5470	0.4704	0.9714	8.3193
323	0.4132	0.8483	0.4703	0.9963	9.0801	0.5977	0.7877	0.5011	0.9905	11.9362	0.5763	0.4108	0.3456	0.9770	14.5110

Table 3
Isotherm parameters for metal ions adsorption onto RHA at different temperatures

Temperature (K)	Cd(II)–RHA				Ni(II)–RHA				Zn(II)–RHA			
	K_F [(mmol/g)/(mmol/dm^3)$^{1/n}$]	$1/n$	R^2	MPSD	K_F [(mmol/g)/(mmol/dm^3)$^{1/n}$]	$1/n$	R^2	MPSD	K_F [(mmol/g)/(mmol/dm^3)$^{1/n}$]	$1/n$	R^2	MPSD
Freundlich												
293	0.0316	0.7556	0.9181	28.6798	0.0483	0.7228	0.8998	30.8847	0.0840	0.5242	0.9647	24.7675
303	0.0355	0.7563	0.9140	30.0835	0.0637	0.6756	0.9155	32.8139	0.1099	0.4890	0.9202	27.8520
313	0.0503	0.6608	0.9214	31.5304	0.0825	0.5984	0.9354	27.9679	0.1325	0.4416	0.9214	28.6951
323	0.0720	0.5453	0.9325	22.2409	0.1147	0.5233	0.8891	30.5420	0.1533	0.4146	0.8845	31.8880

Temperature (K)	Cd(II)–RHA				Ni(II)–RHA				Zn(II)–RHA			
	q_m (mmol/g)	K_L (dm^3/mmol)	R^2	MPSD	q_m (mmol/g)	K_L (dm^3/mmol)	R^2	MPSD	q_m (mmol/g)	K_L (dm^3/mmol)	R^2	MPSD
Langmuir												
293	0.1217	0.3931	0.9663	21.5060	0.2489	0.2682	0.9612	22.9180	0.2313	0.6793	0.9942	13.4383
303	0.1320	0.4127	0.9655	22.5050	0.2702	0.3511	0.9764	23.9298	0.2461	1.0814	0.9908	14.9976
313	0.1347	0.6991	0.9796	22.4243	0.2778	0.4938	0.9878	17.0812	0.2584	1.5341	0.9951	14.3281
323	0.1468	1.2128	0.9851	15.1735	0.2839	0.8897	0.9763	20.3672	0.2656	2.1999	0.9872	19.3930

Temperature (K)	Cd(II)–RHA				Ni(II)–RHA				Zn(II)–RHA			
	K_T (dm^3/mmol)	B_1	R^2	MPSD	K_T (dm^3/mmol)	B_1	R^2	MPSD	K_T (dm^3/mmol)	B_1	R^2	MPSD
Temkin												
293	4.7283	0.0251	0.9793	21.3838	2.8459	0.0553	0.9707	20.5212	6.7054	0.0511	0.9969	11.0110
303	4.8981	0.0275	0.9795	19.1912	3.4832	0.0616	0.9837	14.0866	9.7061	0.0559	0.9795	15.1651
313	6.8385	0.0308	0.9859	13.5086	4.6530	0.0637	0.9895	11.6231	14.6027	0.0563	0.9799	16.8451
323	11.2180	0.0335	0.9767	19.9705	7.5584	0.0669	0.9613	19.6972	20.9611	0.0568	0.9571	21.7244

Temperature (K)	Cd(II)–RHA					Ni(II)–RHA					Zn(II)–RHA				
	K_R (dm^3/g)	a_R (dm^3/mmol)	β	R^2	MPSD	K_R (dm^3/g)	a_R (dm^3/mmol)	β	R^2	MPSD	K_R (dm^3/g)	a_R (dm^3/mmol)	β	R^2	MPSD
R–P															
293	0.0432	0.3044	0.9990	0.9576	19.6787	0.0588	0.2011	0.9990	0.9499	20.3073	0.1480	0.6146	0.9990	0.9931	12.7966
303	0.0488	0.3135	0.9990	0.9556	20.3870	0.0816	0.2555	0.9990	0.9648	20.3896	0.2291	0.8522	0.9990	0.9849	10.8180
313	0.0814	0.5171	0.9990	0.9692	19.0548	0.1215	0.3918	0.9990	0.9815	14.3309	0.3393	1.2189	0.9990	0.9905	9.7830
323	0.1622	1.0388	0.9990	0.9829	13.8395	0.2086	0.6531	0.9990	0.9664	15.1370	0.4618	1.5852	0.9990	0.9792	11.3083

Temperature (K)	Cd(II)–RHA					Ni(II)–RHA					Zn(II)–RHA				
	q_e^∞ (mmol/g)	K_{Th} [(mmol/dm^3)Th]	Th	R^2	MPSD	q_e^∞ (mmol/g)	K_{Th} [(mmol/dm^3)Th]	Th	R^2	MPSD	q_e^∞ (mmol/g)	K_{Th} [(mmol/dm^3)Th]	Th	R^2	MPSD
Toth															
293	0.1375	3.7844	1.1029	0.9569	19.2268	0.1850	7.5405	1.6530	0.9764	16.5890	0.1787	2.1289	1.9196	0.9889	10.6321
303	0.1559	3.2143	1.0025	0.9556	20.3580	0.1980	7.9401	2.0527	0.9933	13.0045	0.1821	1.3140	3.4583	0.9905	10.1467
313	0.1783	2.1402	0.9525	0.9636	19.8701	0.2038	8.1052	2.8104	0.9973	4.7015	0.1923	0.4195	3.4534	0.9836	13.1356
323	0.2134	1.0283	0.6952	0.9726	12.8171	0.2408	2.9724	2.4939	0.9960	9.1846	0.2248	0.3774	2.4736	0.9964	9.3105

The Temkin isotherm is given as:

$$q_e = B_1 \ln(K_T C_e) \quad (8)$$

Temkin isotherm [35] equation contains a factor that explicitly takes into the account the adsorbing species–adsorbent interactions. A plot of q_e versus $\ln C_e$ enables the determination of the isotherm constants B_1 and K_T from the slope and the intercept, respectively. K_T is the equilibrium binding constant (dm^3/mol) corresponding to the maximum binding energy and constant B_1 is related to the heat of adsorption.

Toth isotherm [36] is derived from the potential theory and is applicable to heterogeneous adsorption. It assumes a quasi-Gaussian energy distribution. Most sites have adsorption energy lower than the peak or maximum adsorption energy:

$$q_e = \frac{q_e^{\infty} C_e}{[K_{Th} + C_e^{Th}]^{1/Th}} \quad (9)$$

where q_e^{∞} is the maximum monolayer adsorption capacity parameter (mmol/g), K_{Th} the Toth isotherm constant ((mmol/dm^3)Th) and Th is the dimensionless constant, usually less than unity. The parameters K_{Th} and Th are specific for adsorbate–adsorbent systems. More the parameter Th is away from unity, the more heterogeneous is the system. The parameters K_{Th} and Th are specific for adsorbate–adsorbent systems.

The parameters of the isotherms and the correlation coefficient, R^2, as determined by using the solver add-in function of the MS Excel, for the fitting of the experimental data are listed in Tables 2 and 3. By comparing the results of the values for the MPSD error function and the correlation coefficients (Tables 2 and 3), it is found that the Toth isotherm best represents the equilibrium adsorption of metal ions onto both BFA and RHA.

3.4. Estimation of thermodynamic parameters

The Gibbs free energy change of the adsorption process is related to the equilibrium constant by the classical Van't Hoff equation:

$$\Delta G_0 = -RT \ln K_D \quad (10)$$

The Gibbs free energy change is also related to the entropy change and heat of adsorption at constant temperature according to the following equation:

$$\Delta G_0 = \Delta H_0 - T\,\Delta S_0 \quad (11)$$

Combining the above two equations, one gets:

$$\ln K_D = \frac{-\Delta G_0}{RT} = \frac{\Delta S_0}{R} - \frac{\Delta H_0}{R}\frac{1}{T} \quad (12)$$

where ΔG_0 is the free energy change (kJ/mol), ΔH_0 the change in enthalpy (kJ/mol), ΔS_0 the entropy change (kJ/mol K), T the absolute temperature (K), R the universal gas constant (8.314×10^{-3} kJ/mol K) and K_D ($=q_e/C_e$) is the single point or linear sorption distribution coefficient. Thus, ΔH_0 is the enthalpy change (kJ/mol) which can be determined from the slope of the linear Van't Hoff plot, i.e. $\ln K_D$ versus $(1/T)$, using the equation:

$$\Delta H_0 = \left[R\frac{\mathrm{d}\ln K_D}{\mathrm{d}(1/T)}\right] \quad (13)$$

This ΔH_0 corresponds to the isosteric heat of adsorption ($\Delta H_{st,0}$) with zero surface coverage (i.e. $q_e = 0$) [37]. K at $q_e = 0$ was obtained from the intercept of the $\ln q_e/C_e$ versus q_e plot. Fig. 5 shows the Van't Hoff plot from which ΔH_0 and ΔS_0 values have been estimated (Table 4).

For significant adsorption to occur, the free energy change of adsorption, ΔG_0, must be negative. The thermodynamic relation between ΔF_0, ΔH_0 and ΔS_0 suggests that either (i) ΔH_0 and ΔS_0 are positive and that the value of $T\,\Delta S$ is much larger than ΔH_0, or (ii) ΔH_0 is negative and ΔS_0 is positive or that the value of ΔH_0 is more than $T\,\Delta S$. The adsorption of Cd(II), Ni(II) and Zn(II) onto BFA and RHA is endothermic in nature, giving a positive value of ΔH_0. Hence, ΔS_0 has to be positive and that the positive value of $T\,\Delta S$ has to be larger than ΔH_0. The adsorption process in the solid–liquid system is a combination of two processes: (a) the desorption of the solvent (water) molecules previously adsorbed, and (b) the adsorption of the adsorbate species. The metal ions have to displace more than one water molecule for their adsorption and this results in the endothermicity of the adsorption process. Therefore, ΔH_0 will be positive. The positive value of ΔS_0 suggests increased randomness at the solid/solution interface with some structural changes in the adsorbate and the adsorbent and an affinity of the adsorbents towards Cd(II), Ni(II) and Zn(II) ions. The positive ΔS_0 value also corresponds to an increase in the degree of freedom of the adsorbed species [38]. ΔG_0 values were negative indicating that the sorption process led to a decrease in Gibbs free energy and that the adsorption process is feasible and spontaneous.

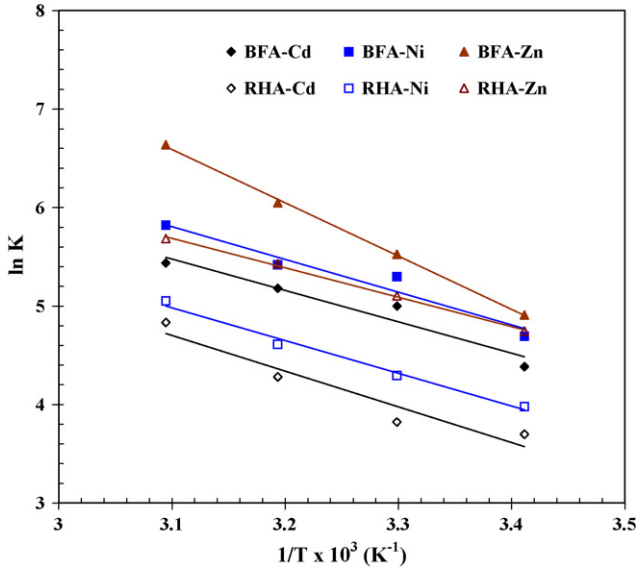

Fig. 5. Van't Hoff plot of adsorption equilibrium constant K.

Table 4
Thermodynamic parameters of the adsorption of metal ions by BFA and RHA (Method III)

Temperature (K)	Cd(II)–BFA				Ni(II)–BFA				Zn(II)–BFA			
	K_D (dm^3/g)	ΔG_0 (kJ/mol)	ΔH_0 (kJ/mol)	ΔS_0 (kJ/mol K)	K_D (dm^3/g)	ΔG_0 (kJ/mol)	ΔH_0 (kJ/mol)	ΔS_0 (kJ/mol K)	K_D (dm^3/g)	ΔG_0 (kJ/mol)	ΔH_0 (kJ/mol)	ΔS_0 (kJ/mol K)
293	0.0801	−10.6835	26.4879	127.6412	0.1093	−11.4411	27.6202	133.8846	0.1355	−11.9648	44.9517	194.1246
303	0.1484	−12.6022			0.2003	−13.3581			0.2508	−13.9248		
313	0.1774	−13.4826			0.2258	−14.1107			0.4236	−15.7488		
323	0.2299	−14.6097			0.3367	−15.6348			0.7630	−17.8328		
Temperature (K)	Cd(II)–RHA				Ni(II)–RHA				Zn(II)–RHA			
	K_D (dm^3/g)	ΔG_0 (kJ/mol)	ΔH_0 (kJ/mol)	ΔS_0 (kJ/mol K)	K_D (dm^3/g)	ΔG_0 (kJ/mol)	ΔH_0 (kJ/mol)	ΔS_0 (kJ/mol K)	K_D (dm^3/g)	ΔG_0 (kJ/mol)	ΔH_0 (kJ/mol)	ΔS_0 (kJ/mol K)
293	0.0432	−9.1786	40.2082	166.8880	0.0585	−9.9171	37.9317	162.8250	0.2007	−12.9218	33.3478	157.8861
303	0.0488	−9.8003			0.0885	−11.2988			0.3101	−14.4601		
313	0.0898	−11.7107			0.1437	−12.9343			0.5160	−16.2624		
323	0.1963	−14.1854			0.2487	−14.8214			0.6931	−17.5746		

3.5. Isosteric heat of adsorption

Apparent isosteric heat of adsorption ($\Delta H_{st,a}$) at constant surface coverage (q_e = 5, 10, 15, 20, 25 mmol/g for BFA and q_e = 3, 6, 9, 12, 15 mmol/g for RHA) is calculated using the Clausius–Clapeyron equation [39]:

$$\frac{d \ln C_e}{dT} = \frac{-\Delta H_{st,a}}{RT^2} \tag{14}$$

or

$$\Delta H_{st,a} = R \left. \frac{d \ln C_e}{d(1/T)} \right|_{q_e} \tag{15}$$

For this purpose, the equilibrium concentration (C_e) at constant amount of adsorbed metal ions is obtained from the adsorption isotherm data at different temperatures. $\Delta H_{st,a}$ is calculated from the slope of the $\ln C_e$ versus $(1/T)$ plot for different amounts of Cd(II), Ni(II) and Zn(II) ions onto BFA and RHA. The isosteres corresponding to different equilibrium adsorption uptake of Cd(II) by BFA and RHA are shown in Figs. 6 and 7, respectively. Similar isosteres were obtained for other systems as well. The linear regression correlation coefficients of the isosteres and the corresponding isosteric enthalpies for all the metal ions and the two adsorbents are presented in Table 5.

The results shown in Table 5 suggest that Eq. (15) represents the experimental data very well. The variation of $\Delta H_{st,a}$ of the six adsorbate–adsorbent systems with the surface loading is presented in Fig. 8. The $\Delta H_{st,a}$ is high at very low coverage and decreases steadily with an increase in q_e indicating that the BFA and RHA have energetically heterogeneous surfaces. The dependence of heat of adsorption with surface coverage is usually observed to display the adsorbent–adsorbate interaction followed by the adsorbate–adsorbate interaction. The adsorbent–adsorbate interaction takes place initially at lower q_e values resulting in high heats of adsorption. On the other

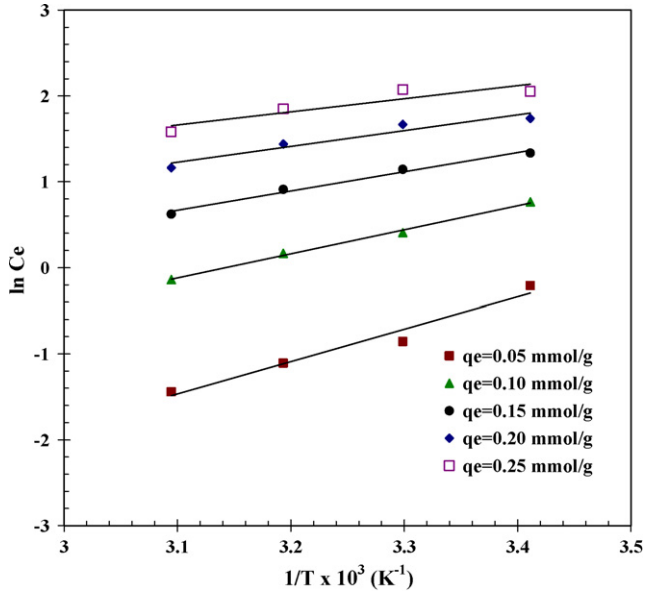

Fig. 6. Adsorption isosters for determining isosteric heat of adsorption for Cd(II)–BFA system.

Table 5
Isosteric enthalpy of metal adsorption onto BFA and RHA

q_e (mmol/g)	Cd(II)–BFA			Ni(II)–BFA			Zn(II)–BFA		
	$\Delta H_{st,a}$ (kJ/mol)	$\Delta H_{st,net}$ (kJ/mol)	R^2	$\Delta H_{st,a}$ (kJ/mol)	$\Delta H_{st,net}$ (kJ/mol)	R^2	$\Delta H_{st,a}$ (kJ/mol)	$\Delta H_{st,net}$ (kJ/mol)	R^2
BFA									
0.05	31.2643	41.7561	0.9826	33.2631	43.7549	0.9853	55.6625	66.1543	0.9985
0.10	23.2761	33.7679	0.9980	23.7241	34.2159	0.9985	35.6440	46.1358	0.9949
0.15	18.6033	29.0951	0.9925	18.1441	28.6359	0.9974	23.9339	34.4257	0.9861
0.20	15.2878	25.7796	0.9646	14.1851	24.6769	0.9762	15.6255	26.1173	0.9632
0.25	12.7162	23.2080	0.9122	11.1142	21.6060	0.9243	9.1810	19.6728	0.8929
q_e (mmol/g)	Cd(II)–RHA			Ni(II)–RHA			Zn(II)–RHA		
	$\Delta H_{st,a}$ (kJ/mol)	$\Delta H_{st,net}$ (kJ/mol)	R^2	$\Delta H_{st,a}$ (kJ/mol)	$\Delta H_{st,net}$ (kJ/mol)	R^2	$\Delta H_{st,a}$ (kJ/mol)	$\Delta H_{st,net}$ (kJ/mol)	R^2
RHA									
0.03	40.3096	50.8014	0.9513	39.6433	50.1351	0.9850	42.7210	53.2128	0.9997
0.06	31.0254	41.5172	0.9617	30.0191	40.5109	0.9860	33.2686	43.7604	0.9990
0.09	25.5944	36.0862	0.9703	24.3893	34.8811	0.9864	27.7392	38.2310	0.9977
0.12	21.7411	32.2329	0.9781	20.3949	30.8867	0.9861	23.8161	34.3079	0.9957
0.15	18.7523	29.2441	0.9851	17.2966	27.7884	0.9852	20.7731	31.2649	0.9930

hand, adsorbate–adsorbate interaction occurs with an increase in the surface coverage. The variation in $\Delta H_{st,a}$ with surface loading can also be attributed to the possibility of having lateral interactions between adsorbed metal ions.

The apparent isosteric heat of adsorption in aqueous solutions, $\Delta H_{st,a}$, is the resultant of the net isosteric heat of adsorption $\Delta H_{st,net}$, heat of solution ΔH_{sol}, and the heat of adsorption of water, ΔH_w, i.e.,

$$\Delta H_{st,a} = \Delta H_{st,net} - \Delta H_{sol} - f\,\Delta H_w \quad (16)$$

where f is the exchange of number of moles of water per mole of adsorbate at the adsorption site. ΔH_w is normally assumed to be zero and ΔH_{sol} of the adsorbate in the solvent may be calculated from the heats of formation data. Since ΔH_{sol} of $3CdSO_4{\cdot}8H_2O$, $NiCl_2{\cdot}6H_2O$ and $ZnSO_4{\cdot}7H_2O$ is 10.4918, −4.807 and −17.974 kJ/mol, respectively, and ΔH_w may be negligible, $\Delta H_{st,net}$ can be calculated from Eq. (16). The calculated values of $\Delta H_{st,net}$ are given in Table 5.

Surface heterogeneity as well as the adsorbate–adsorbate interaction has been taken into account by a new isotherm proposed by Do and Do [40]. This equation is based on the assumptions that the: (a) concerned adsorption system exhibits Type I isotherm, (b) Henry's region exists at zero adsorbate loading, (c) patterns as well as the extent of surface heterogeneity of the adsorbent represented by the isosteric enthalpy of adsorption are independent of the adsorbate, and (d) energy of the adsorbate–adsorbate interaction is a linear function of the adsorption loading. This model takes the enthalpy as a function of the fractional loading of the adsorbate ($\theta = q/q_m$) as shown

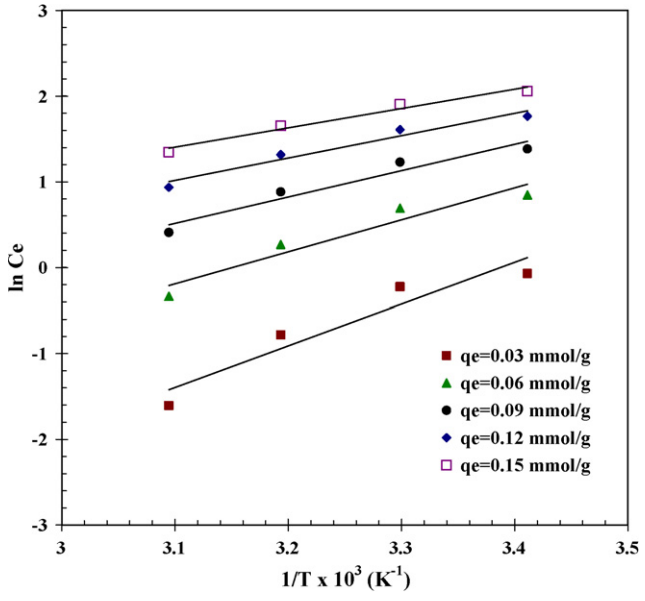

Fig. 7. Adsorption isosters for determining isosteric heat of adsorption for Cd(II)–RHA system.

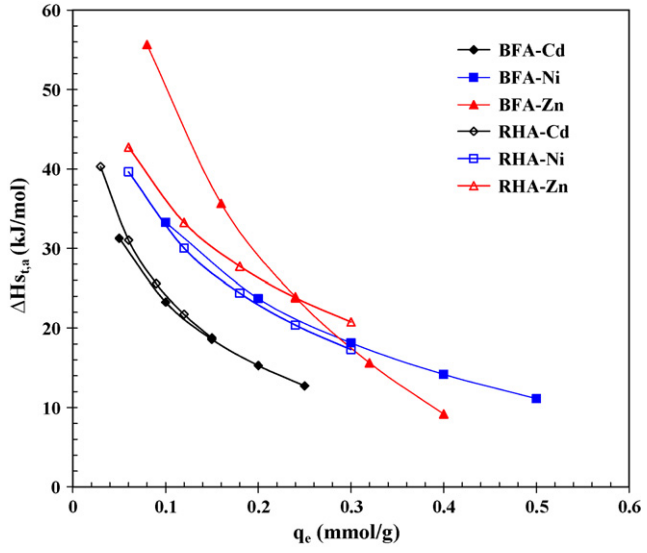

Fig. 8. Variation of $\Delta H_{st,a}$ with respect to surface loading.

Table 6
Non-linear results of isosteric enthalpy of metal adsorption onto BFA and RHA

Adsorbate	$\Delta H_{0,D}$ (kJ/mol)	α	β	μ	MPSD
BFA					
Cadmium	50.7617	0.6302	4.7501	−4.8249	0.0782
Nickel	56.4941	0.6698	4.5849	−5.5058	0.0971
Zinc	104.1624	0.7843	5.1060	−13.2311	0.1608
RHA					
Cadmium	64.4178	0.6284	5.0897	−4.8116	0.9589
Nickel	62.0898	0.6199	4.6179	−5.5313	0.1335
Zinc	58.3366	0.3867	5.2939	−13.4215	0.5014

below:

$$\Delta H = \Delta H_{0,D}\left\{1 - \frac{\alpha\beta\theta}{1+(\beta-1)\theta}\right\} + \mu\theta \quad (17)$$

where $\Delta H(\theta)$ is the isosteric enthalpy corresponding to the fractional loading of adsorbate, θ, and $\Delta H_{0,D}$ is the isosteric enthalpy at zero loading calculated using Do and Do model, which could be termed initial isosteric enthalpy. α is defined as:

$$\alpha = \frac{\Delta H}{\Delta H_{0,D}} < 1 \quad (18)$$

and it represents the ratio of the variation of the isosteric enthalpy with the fractional loading from zero to monolayer coverage (ΔH), and $\Delta H_{0,D}$, and is independent of the adsorbate; β the pattern parameter which characterizes the pattern of surface heterogeneity; μ is the interaction energy of the adsorbed adsorbate molecules between them and is independent of the adsorbent. α reflects the extent of the energy heterogeneity of the surface, which should be free from the adsorbate. The larger the value of α, the greater the extent of surface energy heterogeneity.

For a particular sorption system, ΔH_0 can be directly figured out from the isoster and θ can be calculated from the measured adsorbed quantity of the adsorbate and the maximum adsorption capacity can be obtained from the extrapolation of the well-fitted isotherm if monolayer adsorption is assumed to occur. The other four parameters, isosteric enthalpy at zero loading $\Delta H_{0,D}$, surface heterogeneity factor α, surface heterogeneous pattern characteristic parameter β, and the interaction energy of the adsorbed adsorbate μ, can be estimated by non-linear fitting of the experimental isosteric enthalpy to Eq. (17). The isosteric enthalpy and the corresponding fractional loading have been fitted to Eq. (17) with MS Excel, and the values of $\Delta H_{0,D}$, α, β, and μ for the six adsorbate–adsorbent systems have been obtained and shown in Table 6. The μ values are found to be similar for any of the metal ions onto BFA or RHA with little variation in their values suggesting that the fitting results are reliable. Greater values of α for metal–BFA systems suggest that the BFA has greater surface energy heterogeneity than RHA.

4. Conclusions

The present study shows that the bagasse fly ash (BFA) and rice husk ash (RHA) are effective adsorbents for the removal of cadmium (Cd(II)), nickel (Ni(II)) and zinc (Zn(II)) metal ions from aqueous solutions. Equilibrium isotherms were analyzed by different isotherm models using non-linear regression technique. Toth isotherm is found to represent the equilibrium adsorption of metal ions onto BFA and RHA at all temperatures. Adsorption of metal ions onto BFA and RHA is favourably influenced by an increase in the temperature of the operation. The enhanced sorption at higher temperature indicates endothermic adsorption process. The negative value of ΔG_0 indicates spontaneous adsorption of metal ions onto adsorbents. The isosteric heats of adsorption, $\Delta H_{st,a}$, were calculated by applying the Clausius–Clapeyron equation. The $\Delta H_{st,a}$ was highest at low levels of surface coverage and decreased steadily indicating that the adsorbents, BFA and RHA, possessed heterogeneous surface. The surface heterogeneity of adsorbents could be quantitatively described with an isosteric enthalpy function of fractional loading based on Do's model. The results indicate that the BFA has greater surface heterogeneity than RHA. These results indicate that the use of locally available, almost free of cost, BFA and RHA could be viable alternatives to the activated carbon for the removal of metal ions from aqueous solutions.

Acknowledgement

Authors are thankful to the Ministry of Human Resource Development, Government of India, for providing financial support to undertake the work.

References

[1] W. Rudzinski, D.H. Elserett, Adsorption of Gases on Heterogeneous Surfaces, Academic Press, London, 1991.
[2] R.D. Johnson, F.H. Arnold, The Temkin isotherm describes heterogeneous protein adsorption, Biochim. Biophys. Acta 1247 (1995) 293–297.
[3] B.J. Stanley, J. Krance, A. Roy, Determination of the thermodynamic contribution to peak asymmetry of basic solutes in reversed-phase liquid chromatography, J. Chromatogr. A 865 (1999) 97–109.
[4] A. Geng, K.C. Loh, Heterogeneity of surface energies in reversed-phase perfusive packings, J. Colloid Interf. Sci. 239 (2001) 447–457.
[5] P. Podkoscielny, A. Dabrowski, O.V. Marijuk, Heterogeneity of active carbons in adsorption of phenol aqueous solutions, Appl. Surf. Sci. 205 (2003) 297–303.
[6] V.C. Srivastava, I.D. Mall, I.M. Mishra, Modelling individual and competitive adsorption of cadmium(II) and zinc(II) metal ions from aqueous solution onto bagasse fly ash, Sep. Sci. Technol. 41 (2006) 1–26.
[7] J.W. Patterson, Waste Water Treatment, Science Publishers, New York, 1977.
[8] S.P. Mishra, D. Tiwari, R.S. Dubey, The uptake behaviour of rice (jaya) husk in the removal of Zn(II) ions. A radiotracer study, Appl. Radiat. Isotopes 48 (7) (1997) 877–882.
[9] MINAS Pollution control acts, rules, notification issued there under central pollution control Board, Ministry of Environment and Forests, Government of India, New Delhi, 2001.
[10] World Health Organization, International Standards for Drinking Water, World Health Organization, Geneva, 1993.
[11] V.C. Srivastava, I.D. Mall, I.M. Mishra, Treatment of pulp and paper mill wastewaters with poly aluminium chloride and bagasse fly ash, Colloid Surf. A: Physicochem. Eng. Aspects 260 (2005) 17–28.
[12] I.D. Mall, V.C. Srivastava, N.K. Agarwal, I.M. Mishra, Adsorptive removal of malachite green dye from aqueous solution by bagasse fly ash and activated carbon—kinetic study and equilibrium isotherm analyses, Colloid Surf. A: Physicochem. Eng. Aspects 264 (2005) 17–28.

[13] I.D. Mall, V.C. Srivastava, N.K. Agarwal, I.M. Mishra, Removal of congo red from aqueous solution by bagasse fly ash and activated carbon: kinetic study and equilibrium isotherm analyses, Chemosphere 61 (2005) 492–501.
[14] D.H. Lataye, I.M. Mishra, I.D. Mall, Removal of pyridine from aqueous solution by adsorption on bagasse fly ash, Ind. Eng. Chem. Res. 45 (11) (2006) 3934–3943.
[15] V.C. Srivastava, M.M. Swamy, I.D. Mall, B. Prasad, I.M. Mishra, Adsorptive removal of phenol by bagasse fly ash and activated carbon: equilibrium, kinetics and thermodynamics, Colloid Surf. A: Physicochem. Eng. Aspects 272 (1–2) (2006) 89–104.
[16] V.C. Srivastava, I.D. Mall, I.M. Mishra, Equilibrium modelling of single and binary adsorption of cadmium and nickel onto bagasse fly ash, Chem. Eng. J. 117 (1) (2006) 79–91.
[17] IS 1350 part I, Methods of test for coal and coke, proximate analysis, Bureau of Indian Standards, Manak Bhawan, New Delhi, India, 1984.
[18] IS 355, Methods of determination of chemical composition of ash of coal and coke, Bureau of Indian Standards, Manak Bhawan, New Delhi, India, 1974.
[19] E.P. Barret, L.G. Joyner, P.P. Halenda, The determination of pore volume and area distributions in porous substances. 1. Computations from nitrogen isotherms, J. Am. Chem. Soc. 73 (1951) 373–380.
[20] D.W. Marquardt, An algorithm for least-squares estimation of non-linear parameters, J. Soc. Ind. Appl. Math. 11 (1963) 431–441.
[21] V.C. Srivastava, I.D. Mall, I.M. Mishra, Characterization of mesoporous rice husk ash (RHA) and adsorption kinetics of metal ions from aqueous solution onto RHA, J. Hazard. Mater. B 134 (2006) 257–267.
[22] S. Brunauer, L.S. Deming, W.E. Deming, E. Teller, J. Am. Chem. Soc. 62 (1940) 1723.
[23] K.S.W. Sing, Adsorption methods for the characterization of porous materials, Adv. Colloid Interf. Sci. 76–77 (1998) 3–11.
[24] IUPAC Manual of Symbols and Terminology of Colloid Surface, Butterworths, London, 1982.
[25] S.R. Kamath, A. Proctor, Silica gel from rice hull ash: preparation and characterization, Cereal Chem. 75 (1998) 484–487.
[26] M.M. Abou-Mesalam, Sorption kinetics of copper, zinc, cadmium and nickel ions on synthesized silico-antimonate ion exchanger, Colloid Surf. A: Physicochem. Eng. Aspects 225 (2003) 85–94.
[27] M.M. Davila-Jimenez, M.P. Elizalde-Gonzalez, A.A. Pelaez-Cid, Adsorption interaction between natural adsorbents and textile dyes in aqueous solution, Colloid Surf. A: Physicochem. Eng. Aspects 254 (2005) 107–114.
[28] S. Ricordel, S. Taha, I. Cisse, G. Dorange, Heavy metals removal by adsorption onto peanut husks carbon: characterization, kinetic study and modeling, Sep. Purif. Technol. 24 (2001) 389–401.
[29] A. Saeed, M. Iqbal, M.W. Akhtar, Removal and recovery of lead(II) from single and multimetal (Cd, Cu, Ni, Zn) solutions by crop milling waste (black gram husk), J. Hazard. Mater. B 117 (2005) 65–73.
[30] G. McKay, J.F. Porter, Equilibrium parameters for the sorption of copper, cadmium and zinc ions onto peat, J. Chem. Technol. Biotechnol. 69 (3) (1997) 309–320.
[31] F. Pagnanelli, A. Esposito, L. Toro, F. Veglio, Metal speciation and pH effect on Pb, Cu, Zn and Cd biosorption onto *Sphaerotilus natans*: Langmuir-type empirical model, Water Res. 37 (3) (2003) 627–633.
[32] H.M.F. Freundlich, Over the adsorption in solution, J. Phys. Chem. 57 (1906) 385–471.
[33] I. Langmuir, The adsorption of gases on plane surfaces of glass, mica and platinum, J. Am. Chem. Soc. 40 (1918) 1361–1403.
[34] O. Redlich, D.L. Peterson, A useful adsorption isotherm, J. Phys. Chem. 63 (1959) 1024–1026.
[35] M.J. Tempkin, V. Pyzhev, Acta Physiochim. URSS 12 (1940) 217–222.
[36] J. Toth, State equations of the solid gas interface layer, Acta. Chem. Acad. Hung. 69 (1971) 311–317.
[37] M. Suzuki, T. Fujii, Concentration dependence of surface diffusion coefficient of propionic acid in activated carbon particles, AIChE J. 28 (1982) 380–385.
[38] C. Raymon, Chemistry: Thermodynamic, McGraw-Hill, Boston, 1998, p. 737.
[39] D.M. Young, A.D. Crowell, Physical Adsorption of Gases, Butterworths, London, 1962, p. 426.
[40] D.D. Do, H.D. Do, A new adsorption isotherm for heterogeneous adsorbent based on the isosteric heat as a function of loading, Chem. Eng. Sci. 52 (2) (1997) 297–310.